Est. 1984

ORIENTAL JOURNAL OF CHEMISTRY
An International Open Access, Peer Reviewed Research Journal

www.orientjchem.org

ISSN: 0970-020 X
CODEN: OJCHEG
2023, Vol. 39, No.(3):
Pg. 703-711

Efficient Removal of Cationic and Anionic Dyes from Synthetic and Real Wastewater by Plant-mediated Nickel Nanoparticles

HARSHVARDHAN CHAUHAN[1]*, MOHD SAQUIB TANWEER[1] and MASOOD ALAM[1]*

[1]Environmental Science Research Lab, Department of Applied Sciences & Humanities, Faculty of Engineering & Technology, Jamia Millia Islamia, New Delhi, 110025, India.
*Corresponding author E-mail: chauhanhvsc@gmail.com, malam@jmi.ac.in

http://dx.doi.org/10.13005/ojc/390321

(Received: April 04, 2023; Accepted: May 10, 2023)

ABSTRACT

In this study, Ni NPs were produced by biosynthesis method with the help of phytoconstituents present in the *Sahadevi* plant *(Vernonia cinerea)* ethanoic extract namely *Sahadevi* nickel nanoparticles (SNPs). SNPs were characterized using XRD, FT-IR, HR-FESEM. XRD study shows crystalline nature of SNPs. SNPs were employed as bioadsorbent for the elimination of dyes like cationic (BG) and anionic (CR) dyes from aqueous media. Adsorption capacity of SNPs was analyzed in batch modes at various pH, initial dye concentration, contact time, isotherm, and kinetics. The maximum adsorption capacity (q_m) shown in Langmuir isotherm was obtained as 1666.7 mg g^{-1} in case of BG dye and 666.7 mg g^{-1} in CR dye, respectively. The higher value of coefficient of Langmuir isotherm recommended monolayer adsorption. Adsorption kinetics information was valuable suited to pseudo-second order kinetics with R^2>0.99 for both dyes. SNPs proved to be an efficient sorbent for the elimination of dyes from aqueous media and can be employed to remove textile and tannery discharges. Overall, this study suggests that the use of SNPs is safe and secure, eco-friendly, cost-effective, which can be used as bioadsorbent removing colored organic effluents as dyes from water bodies.

Keywords: Ni NPs, *Sahadevi* plant *(Vernonia cinerea)* ethanoic extract, Cationic and anionic dyes, Adsorption, Textile water purification.

INTRODUCTION

Copious amounts of colored organic effluents are produced in modern industries like paints, textiles, cosmetics, paper, plastics, etc. Such discharges of colouring effluents in aqueous media in a small amount can distress terrestrial animals and aquatic life. Hence different colouring effluents cannot be liquidated without suitable treatment in the water bodies. Due to their complex orientation and synthetics routes[1], these colouring organic effluents cannot be effortlessly removed or degraded with effluents removing methods. Such dyes are designed to resist disintegration in required amount of time. It means that elimination of dyes has been a vital as well as stimulating area for saving terrestrial animals, aquatic life, and humans.

Dyes have unfriendly impact on individuals' health such as skin irritation, itchy, respiratory disorders, cancer, and watery eyes[2]. Azo dyes having N=N group like methyl orange (MO), Congo red (CR),

are commonly utilised dye which reduce sunlight penetration ultimately affecting aquatic organisms, as well as the photosynthetic process. Azo groups when combine with aromatic amines cause carcinogenic symptoms in humans and as well as other animals[3,4]. Brilliant green (BG) dye is used in medical purposes like veterinary medicines, dermatological agents, and biological stain and it becomes much more hazardous after swallowing, skin contact and eye contact. This may create oxides of sulphur, carbon, and nitrogen after their degradation[5]. The stability of CR dye in light, detergents, and water is not a cause for concern; however, the presence of aromatic amines in the dye's structure, which is responsible for carcinogenesis, poses a significant danger to aquatic life and humans[6,7]. Hence dyes are urgently desired to be taken off from polluted water.

In the recent times, various biological, physico-chemical, physical, and chemical approaches have been exploited for the removal of colouring contaminants and various dyes from industrialized water wastes. Among these approaches, adsorption has been originated to be most prevalent physico-chemical approach for eliminating dyes with probable applications[8] due to operation simplicity, enhanced efficiency, low cost of adsorbent and its design. At present time, it has been testified that several diverse types of effective adsorbents are employed for dyes' elimination from wastewater[9-13].

In the present time, various metallic nanoparticles (MNPs) have been synthesized of varying shapes, sizes, compositions, morphologies, and physio-chemical properties. MNPs have attracted much more attention from scientific community due to their notable properties such as thermal strength, high surface area, mechanical strength, high ordered structure optical[14] and magnetic properties[15]. Recently, experts have noticed it inexpensive to manufacture bio-metallic nanoparticles with the help of livings sources (plants, fungus, and algae), as they are readily available, cost effective, harmless, and competent. In literature it has been reported that many types of MNPs have been employed to sequestrate toxic dyes from the wastewater. For instance, Kumar et al reported that low-cost synthesis of metal oxide nanoparticles (ZnO and SnO_2) could show efficiency for adsorption of commercial dye in aqueous media[16]. Pham *et al.,* concluded that tungsten oxide (H-WO_3) showed adsorption activity towards methylene blue (MB) in acidic media[17].

Numerous applications of plant-mediated developed metal nanoparticles for the elimination of dyes and coloured organic effluents comprising, silver[18], iron oxide and zinc oxide nanoparticles have been testified. Ethanolic extract of plant comprises different secondary metabolites like terpenoids, alkaloids, and flavonoids in which organic compounds are primarily reliable for conversion of ionic to bulk MNPs synthesis[19]. The Ethanolic extract of whole plant has capability of strong reducing, stabilizing, and capping agent. In addition, Nickel nanoparticles are procured for their diverse catalytic and medical purposes[20] including biosorption, antibacterial, cytotoxic, remediation[21], anticancer, antioxidant, and enzyme inhibition properties etc.

Vernonia cinerea, Sahadevi (Sanskrit) plant is a common weed that is found throughout India and belongs to Asteraceae family. This plant is having various curative applications as distinct conventional medicine for the humankind. The *Sahadevi* plants possess antibacterial[22], antioxidant[23], antimicrobial, analgesic, antipyretic, antispasmodic and hepatoprotective properties.

The objective of this paper was to find out the elimination efficiency of colouring organic effluents such as dyes (BG and CR) from the aqueous media with the help of Nickel nanoparticles (Ni NPs) that were synthesized by forest weed ethanol plant extract *(Vernonia cinerea)* in batch equilibrium approach. The current study examines the impact of various factors such as contact time, dye concentration, kinetic study (pseudo-first order and pseudo-second-order model) and adsorption isotherms (Langmuir and Freundlich).

EXPERIMENT

Materials

All the chemicals and reagents were of analytical grade and used without further purification. Stock solutions (1000 mg/L) of CR [$C_{32}H_{22}N_6Na_2O_6S_2$], and BG [$C_{27}H_{34}N_2O_4S$] was made in double distilled water (DDW), Nickel nitrate [$Ni(NO_3)_2 \cdot 6H_2O$], NaOH, HCl, and ethanol were purchased from Merck Company, Chennai, India.

Preparation of *Sahadevi* ethanoic extracts

Firstly, the whole plant of *Sahadevi* was collected from the nursery of Jamia Millia Islamia, New Delhi, India. In the process of obtaining ethanol extract, we followed Joshi *et al.,* approach with some alteration[24]. The collected plant was rinsed several times with tap water to remove its dust particles. Again, it was washed with DDW and dried in shade for 2 weeks to remove moisture contents. Dried leaves were powdered in grinder mixer and stored in dark at room temperature. 2.8 g of air-dried powder mixed with ethanol (500 mL) and kept at room temperature for 5 days. The mixture was heated at low temperature for 30 min using waterbath to find concentrated extract of the plant. Finally, mixture was filtered using Whatman filter paper (pore size: 11µm) and stored at cool place for further applications.

Preparing plant-mediated *Sahadevi* Nickel nanoparticles (SNPs)

5 mM of $Ni(NO_3)_2.6H_2O$ was added in Erlenmeyer flask containing 100 mL DDW, and 10 mL of *Sahadevi* plant extract (as Phyto-reducing agent). It was mixed well using magnetic stirring (800 rpm) at room temperature for 2 hours. Colour change was observed from green to pale yellow indicating the formation of Ni NPs. Precipitate got settled down in flask after completion of the reaction. Mixture was purified by centrifugation (5000 rpm) for 10 mins with DDW and dried at room temperature.

Characterization of SNPs

For the study of surface morphology of SNPs, High Resolution Field Emission Scanning Electron Microscopy (HR-FESEM) (NOVA NANOSEM-450, FEI, Netherlands) were employed. For knowing presence of functional groups on the SNPs surface, recording Fourier Transform Infrared spectrometer (FTIR) (Tensor 37, Bruker) spectra having range 4000 to 400 cm^{-1} consuming KBr was used. For investigating crystalline structure and nature of the phase, X-ray diffraction patterns having high angle range of 7.99°-4° min^{-1}(2Θ)(Rigaku Smart Lab Guidance, Rigaku) (Nano centre JMI New Delhi) had been vested.

Batch adsorption studies

To prepare stock solution, 1 g of both dyes (BG and CR) (analytical grade) was dissolved in 1 L of DDW separately. Entirely, during the batch experimental process for sorption of dyes, proper dilutions were made from the standard solution. Batch adsorption experiments were performed with 0.01 g of SNPs dose and 20 mL of 40 mg L^{-1} of both dyes, and continuously shaking on rotary shaker (200 rpm) for 24 h at 25±2°C. The residual concentration of dyes in preserved water samples were testified by measuring the absorbance of CR and BG dyes at lambda max of 500 and 625nm, respectively. The values of removal efficiency R(%) and dye performance uptake (q_e;mg g^{-1}) were determined by applying the following formulas.

$$R\ (\%) = \frac{C_i - C_e}{C_i} \times 100 \quad (1)$$

$$q_e = \frac{C_i - C_e}{M} \times V \quad (2)$$

Here, M (g) is the amount of the SNPs nanomaterial and `V` is the volume of BG and CR dye solutions as adsorbate in litre(L).

RESULTS AND DISCUSSIONS

Characterization of SNPs

Fourier Transform Infrared Spectroscopy(FTIR)

The vibrational spectra of SNPs and post adsorption of BG and CR dyes were interpreted in the Fig. 1. Spectral lines in FTIR of SNPs produced by ethanoic extract of sahadevi had been properly recognised in the literature. The peak at 3642 cm^{-1} refers to the existence of phenolic (-OH) groups stretching in flavonoids and glycosides in all 3 samples. The phytochemicals having Ether (-O-) as well as methyl (CH_3-) functional groups were confirmed by the emergence of broad peaks at 1109 cm^{-1} [25] and 2861 cm^{-1} as shown in Fig. 1(a).

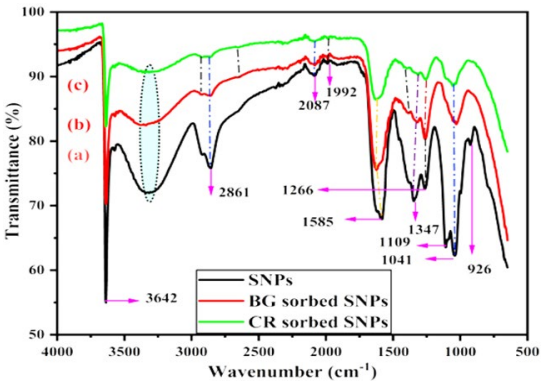

Fig. 1. FTIR spectra of SNPs, (a) BG dye loaded (b), and CR dye loaded (c)

In all three samples, from wavenumber 4000 cm^{-1} to 2983 cm^{-1} there are possibly methyl functional groups engage with dyes in both samples as displayed in Fig. 1(b and c). From 2884 cm^{-1} to 1672 cm^{-1}, the middle range is probably similar in both Fig. 1 (b and c). But SNPs (Fig. 1a) has a change, and 2087 cm^{-1} and 1585 cm^{-1} peak refers to cross-linked C-C stretching as well as phenol rings.

Last part of spectral lines from 1673 cm^{-1} to 654 cm^{-1} having 1109 cm^{-1} and 926 cm^{-1} can be attributed to C-O and C-O-C groups stretching[22]. Fig. 1 b and 1 c show many changes because of sorbed SNPs, proving that adsorption has occurred in respect of both dyes namely BG and CR on SNPs surfaces. Thus, active groups present on SNPs surfaces have modified and improved interactions with dyes.

High-Resolution X-ray Diffraction (XRD)

The crystallinity and phase structure of the Bio-inspired Ni-NPs were recorded by X-ray diffraction (XRD). XRD configurations of SNPs attained by green method have been displayed in Fig. 2. The clear diffraction peaks arising at 47.6°,51.7°, and 75.2° have been indexed as face-centred cubical structure(fcc). All these three peaks correspond to 111, 200, and 220[26] crystal plane (JPCDS:04-0835), respectively.

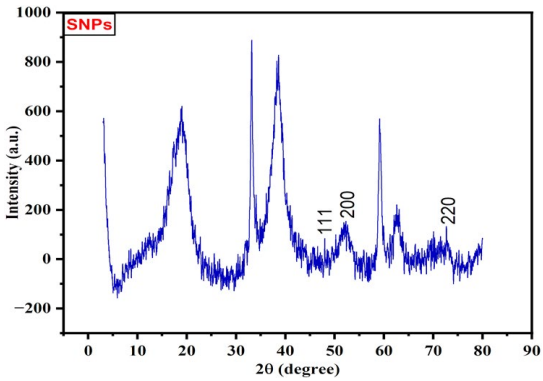

Fig. 2. XRD spectra of SNPs

High Resolution Field Emission Scanning Electron Microscopy(HR-FESEM)

HR-FESEM has been operational as a vital tool for the investigation of bio-inspired Ni nanoparticles (SNPs). Fig. 3 shows HR-FESEM of SNPs and BG/CR absorbed SNPs. HR-FESEM image of SNPs sample disclosed that the surface structure was rough, porous, and cracked (Fig. 3a). In Fig. 3b, HR-FESEM visibly demonstrated that rough, porous, and surface of adsorbent has been filled by adsorption[1] of BG and CR dyes. After dyes adsorption significant morphological changes can be seen in Fig. 3b, as pores and cracked sites have been packed and condensed by both cationic (BG) and anionic (CR) dyes. It shows that biosorption has been occurring between SNPs' surface and BG and CR dyes.

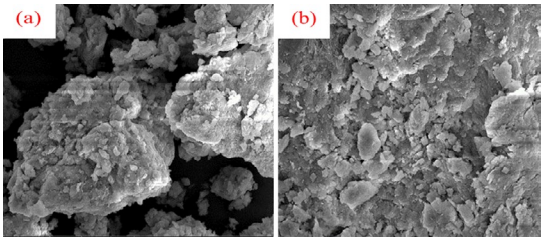

Fig. 3. Surface morphology of SNPs (a), dye sorbed SNPs (b)

Batch experiment

Impact of pH

In the adsorption process, the pH study shows a critical role and reveals the nature of surface binding sites of the adsorbents in aqueous media. The impact of pH (2 to 9) on BG/CR adsorption at room temperature with 0.01 g of SNPs (10 mL) in aqueous adsorbate solutions (BG-10 mg L^{-1} and CR-10 mg L^{-1}) and 120 min contact time is displayed in Fig. 4. The utmost BG and CR dyes elimination commences at pH 8 and 6, respectively. The adsorption capacity of SNPs gets influenced by both degree of ionization of active groups and nature of surface of the adsorbent. The maximum removal efficiency of BG dye is at pH 8 (99.34 %) and pH 6 (99.2 %) in case of CR dye. In basic medium, SNPs and anionic CR dyes build strong electrostatic attraction, and thus successfully removing CR from aqueous solution. Further increase in pH leads to more competition in between the OH^- ions, ultimately reducing the removal efficiency of SNPs. The enhanced adsorption of BG dye at higher pH[12] is due to upsurge in electrostatic attraction between the positively charged BG dye and (-ve) charged surface of SNPs.

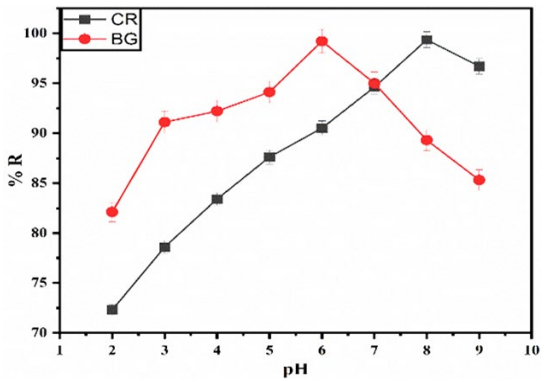

Fig. 4. Impact of pH study

Impact of contact time and kinetics study

In Fig. 5, it is clearly shown that BG and CR uptake (%) onto SNPs adsorbent enhances with the rise in the interaction time. After 120 min the removal was 99% for both cationic BG and anionic CR dyes. Such a good adsorption got boosted by accessibility of functioning adsorptive sites onto SNPs at primary phase technique of adsorption. Two types of kinetic models, i.e., PFO and PSO, were applied for BG and CR dye sorption from the aqueous phase to estimate the adsorption mechanism. Table 1 presents the parameters of selected kinetic models. PSO kinetic is evidently proficient for both cationic and anionic dyes as evaluated q_e value and experimental q_e values are closer. (i.e., for BG: q_e (exp)-297 mgg^{-1}, q_e(cal)- 303.03 mg g^{-1}, and for CR: q_e (exp)-222.75 mg g^{-1}, q_e (cal)-227.27 mg g^{-1}), thus confirming chemisorption is rate verifying step[27].

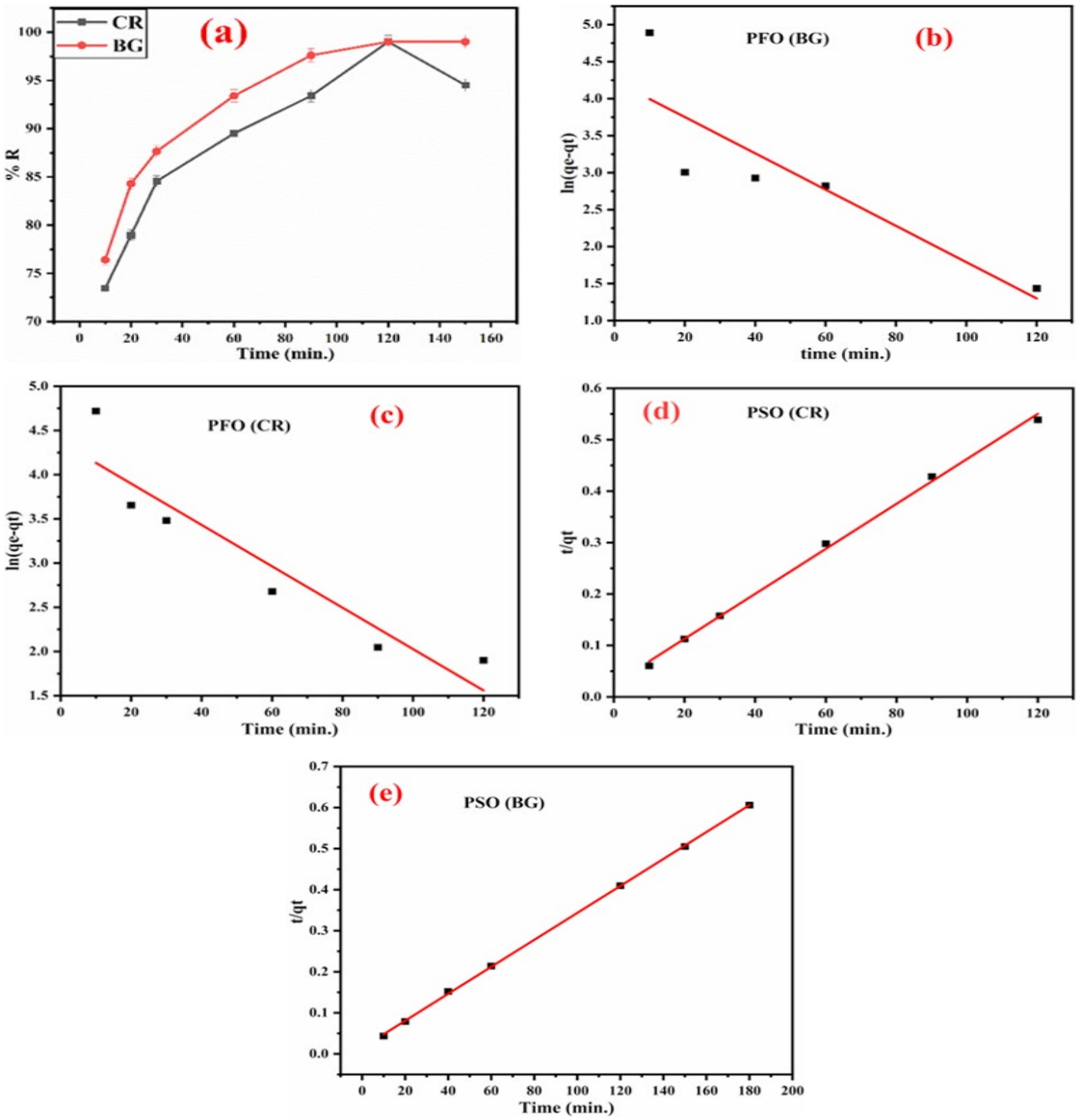

Fig. 5. Impact of contact time (a), Pseudo-first order kinetic model for the sorption of BG dye(b) and CR dye (c); and Pseudo-second order kinetic model of the sorption of CR dye (d) and BG dye (e)

Effect of BG and CR concentration and isotherm study

The result of the doses of BG and CR dyes were studied ranging from 10 mg L^{-1} to 180 mg L^{-1} on SNPs. It is clearly displayed in Fig. 6, that the removal efficiency increases from 86.18 to 99.94% in case

of BG dye, and from 71.1 to 97% of CR dye with the increase in concentration of dyes. Equilibrium reached with 90 mg L^{-1} and 120 mg L^{-1} concentration for BG and CR dyes, respectively. Further, as dyes concentration upsurges, an intense driving force is created that concedes dyes molecules to overwhelm all their resistance shift from the liquid phase to the solid matter. Fig. 6 shows two isotherm models for BG and CR dyes adsorption on the SNPs surface. Table 2 exhibits the parameters of chosen isotherm models. In Langmuir model, the maximum adsorption capacities (q_m) for SNPs have been recorded as 1666.7 and 666.7 mg g^{-1} for BG and CR, respectively. Table 3 shows comparison study for the maximum adsorption capacities of various green synthesized metallic nanoparticles. Separation factor (R_l) lies in the range between 0 to 1 i.e., 0.92 for BG and 0.819 for CR dye.

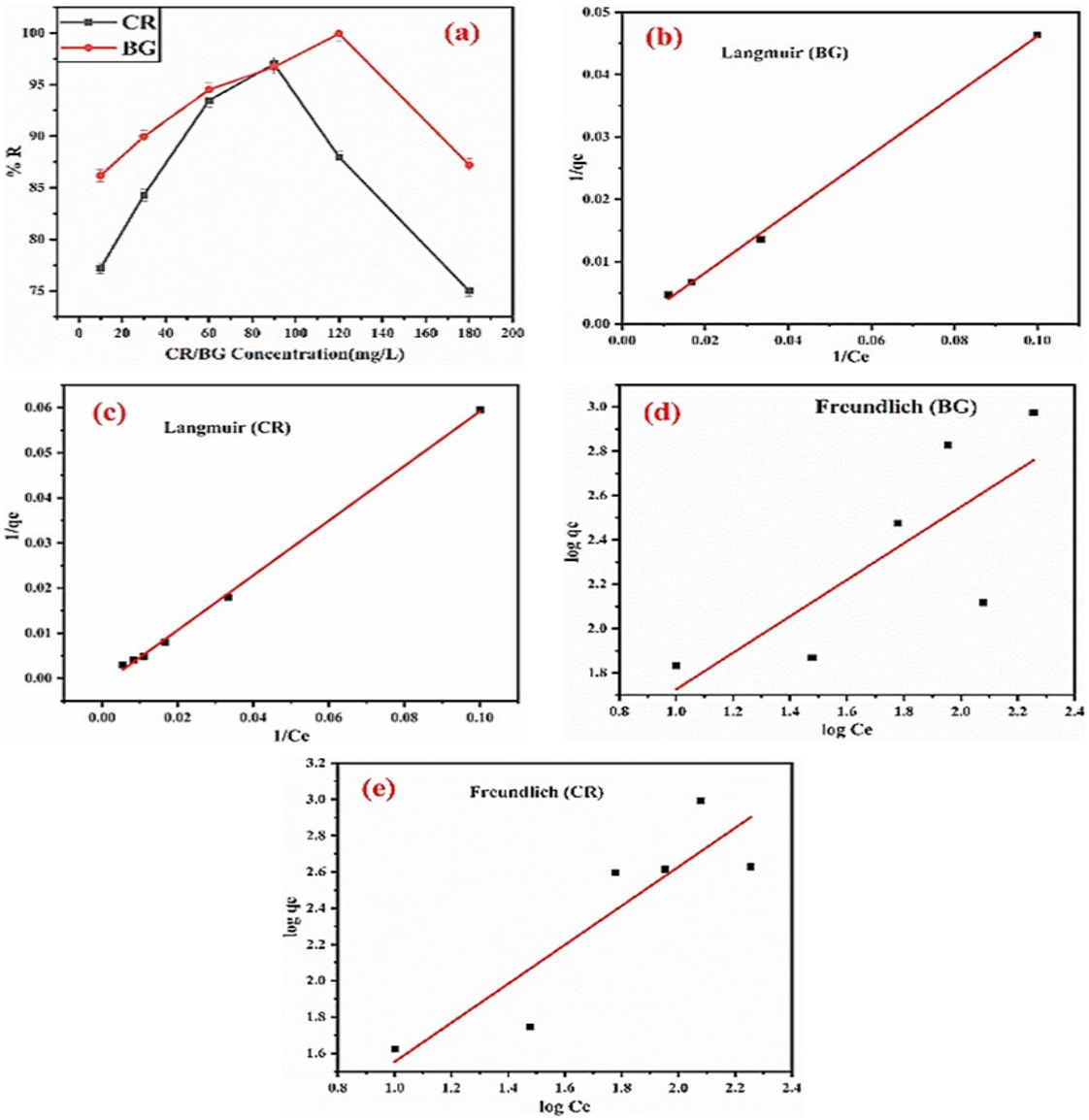

Fig. 6. Effect of initial concentration of CR/BG concentration (a), Langmuir (BG) (b), Langmuir (CR) (c), Freundlich (BG) (d), Freundlich (CR) (e)

Which approves favourable adsorption of BG and CR dye and appropriateness of the Langmuir isotherm model[28].

Application of SNPs towards Real Water Samples

The adsorption efficiency of as prepared SNPs has also been tested by choosing real water

samples including tap water (Department of applied science and humanities, Jamia Millia Islamia, New Delhi, India), river water (Okhla Yamuna, New Delhi, India) and agricultural irrigation water (Tubewell, 27.6712° N, 78.7278° E, Village Abhaypura, District Kasganj U.P). All water samples were investigated separately with diverse concentrations of BG (10, 30, 60, 90,120 and 150 mg L^{-1}) and CR (10, 30, 60, 90, 120, and 150 mg L^{-1}) dyes in ideal conditions. After attainment of equilibrium, the aliquot part of both dyes was collected from reaction beaker using centrifugation and unknown concentration was calculated with the help of ultraviolet–visible (UV–Vis) spectrophotometry. Results are shown in Table 4 with excellent removal efficiency of targeted dyes from real water samples that support the cogency of the synthesized biosorbent (SNPs). Such a behavior may be understood due to the favorable morphological adsorptive sites and functional groups on the exterior surface of the SNPs.

Table 1: Parameters of PFO and PSO models for the sorption of both BG and CR dye on the SNPs

Adsorbent	PFO (BG)				PFO (CR)			
	q_e(exp) (mg g^{-1})	q_e(cal)(mg g^{-1})	K_1(min^{-1})	R^2	q_e(exp) (mg g^{-1})	q_e(cal)(mg g^{-1})	K_1(min^{-1})	R^2
SNPs	297	69.505	8.24E-05	0.754	222.75	42.735	0.00019	0.882
	PSO (BG)				PSO (CR)			
	q_e(exp)(mg g^{-1})	q_e(cal)(mg g^{-1})	K^2(min^{-1})	R^2	q_e(exp)(mg g^{-1})	q_e(cal)(mg g^{-1})	K^2(min^{-1})	R^2
	297	303.03	0.00075	0.999	222.75	227.27	0.00079	0.997

Table 2: Parameters of Langmuir model for the sorption of both BG and CR dye on the SNPs

Adsorbent	Langmuir Model (BG)				Langmuir Model (CR)			
	q_m(mg g^{-1})	K_l(L mg^{-1})	R_l	R^2	q_m(mg g^{-1})	K_l(L mg^{-1})	R_l	R^2
SNPs	1666.7	0.00129	0.93	1	666.7	0.0025	0.82	0.99

Table 3: Comparison of maximum adsorption capacity for various green synthesized metallic nanoparticles

CR dye	Biosorbents	q_m(mg g^{-1})	Ref.
	ZnO NPs	9.615	[29]
	(ZnO)	50	[30]
	$ZnOeCdWO_4$	26.5	[31]
	Sn (II)-BDC MOF	95.2	[32]
	SNPs nanobiosorbent	666.7	Present study
BG dye	Ag NPs	19.26	[33]
	Fe NPs	125	[34]
	Ag NPs	256	[35]
	PAPE/AZO	94.46	[36]
	Fe_3O_4@AC	166.6	[37]
	SNPs biosorbent	1666.7	Present study

Table 4. Removal Efficiency of the SNPs for BG and CR Dyes from Tap Water, Agriculture irrigation water, and River Water

Real water sample	BG(mg L^{-1})	CR(mg L^{-1})	BG(%R)	CR (%R)
Tap water	10	10	85.6	87.6
	30	30	82.3	84.3
	60	60	76.6	79.87
	90	90	71.2	73
	120	120	66.6	68.5
	150	150	62.3	65.5
Agriculture irrigation water	10	10	83.1	84.3
	60	60	74.3	76.7
	30	30	78.8	80
	90	90	70.8	71.2
	120	120	65.4	67.5
	150	150	61.2	64.2
River water	10	10	82.4	83.3
	30	30	78.6	77.7
	60	60	73.2	73.4
	90	90	67.8	69.8
	120	120	62.3	63.4
	150	150	60.3	61.4

CONCLUSION

In this research work, the bio-inspired nickel nanoparticles have been fruitfully synthesized using ethanoic extract of whole plant i.e., *Sahadevi* plant *(Vernonia cinerea)*. It can be employed for colored organic effluents and decolorization of textile discharges containing BG and CR dyes. Biosorption of dyes onto SNPs followed Langmuir isotherm with q_m of 1666.7 mg g^{-1} for BG and 666.7 mg g^{-1} in case of CR dye. Adsorption kinetics study shows that the uptake of dyes onto SNPs is well suited with Pseudo second order. It thus becomes evident that SNPs can be a potential adsorbent material for the deprivation of toxic dyes.

ACKNOWLEDGMENT

One of the authors, Harshvardhan Chauhan is thankful to the University Grants Commission (UGC) for the Non-NET Fellowship.

Conflict of interest

The author declare that we have no conflict of interest.

REFERENCES

1. Bir, R.; Tanweer, M. S.; Singh, M.; Alam, M., *ACS Omega.*, **2022**, *7*(49), 44836–44850.
2. Chung, K.-T., *J. Environ. Sci. Heal. Part C.*, **2016**, *34*(4), 233–261.
3. Brüschweiler, B. J.; Merlot, C., *Regul. Toxicol. Pharmacol.*, **2017**, *88*, 214-226.
4. Shi, Y.; Yang, Z.; Xing, L.; Zhang, X; Li, X; Zhang, D. *World J Microbiol Biotechnol.*, **2021** *37*, 137.
5. Mansour, R. A.; El Shahawy, A.; Attia, A.; Beheary, M. S. *Int. J. Chem. Eng.*, **2020**, 1–12.
6. Bhat, S.A.; Zafar, F.; Mondal, A.H.; Kareem, A.; Mirza, A.U.; Khan, S.; Mohammad, A.; Haq, Q. M. R.; Nishat, N., *J Iran Chem Soc.*, **2020**, *17*, 215–227.
7. Harja, M.; Buema, G.; Bucur, D., *Sci Rep.*, **2022**, *12*, 6087.
8. Bhushan, B.; Nayak, A.; Kotnala, S., *Mater. Today Proc.*, **2021**, *44*, 187–191.
9. Iqbal, Z.; Tanweer, M. S.; Alam, M., *J. Water Process Eng.*, **2022**, *46*, 102641.
10. Samanta, P.; Desai, A. V.; Let, S.; Ghosh, S. K. *ACS Sustain. Chem. Eng.*, **2019**, *7*(8), 7456–7478.
11. Singh, N.; Riyajuddin, S.; Ghosh, K.; Mehta, S. K.; Dan, A. *ACS Appl. Nano Mater.*, **2019**, *2*(11), 7379–7392.
12. Al-Rawashdeh, N. A. F.; Allabadi, O.; Aljarrah, M.T. *ACS Omega.*, **2020**, *5*(43), 28046–28055.
13. Ahmad, S.; Tanweer, M. S.; Mir, T. A.; Alam, M.; Ikram, S.; Sheikh, J. N., *J. Water Process Eng.*, **2023**, *51*, 103377.
14. Banin, U.; Ben-Shahar, Y.; Vinokurov, K. *Chem. Mater.*, **2014**, *26*(1), 97–110.
15. Iqbal, Z.; Tanweer, M. S.; Alam, M., *ACS Omega.,* **2023**, *8*(7), 6376–6390.
16. Kumar, K. Y.; Muralidhara, H. B.; Nayaka, Y. A.; Balasubramanyam, J.; Hanumanthappa, H., *Powder Technol.*, **2013**, *246*, 125–136.
17. Pham, N. L.; Luu, T. L. A.; Nguyen, H. L.; Nguyen, C. T., *Mater. Chem. Phys.*, **2021**, *272*, 125014.
18. Abbasi, M.; Saeed, F.; Rafique, U. *IOP Conf. Ser. Mater. Sci. Eng.*, **2014**, *60*, 012061.
19. Aromal, S. A.; Philip, D. *Spectrochim. Acta Part A Mol. Biomol. Spectrosc.*, **2012**, *97*, 1–5
20. Chauhan, H.; Alam, M., *Springer International Publishing: Cham.*, **2020**, 141–167.
21. Tanweer, M. S.; Chauhan, H.; Alam, M. *Springer Singapore.*, **2022**, 97–124.
22. Anjana, V. N.; Joseph, M.; Francis, S.; Joseph, A.; Koshy, E. P.; Mathew, B. Artif., *Cells, Nanomedicine, Biotechnol.*, **2021**, *49*(1), 438–449.
23. Ramaswamy, U.; Mukundan, D.; Sreekumar, A.; Mani, V. *Mater. Today Proc.*, **2015**, *2*(9), 4600–4608.
24. Joshi, T.; Pandey, S. C.; Maiti, P.; Tripathi, M.; Paliwal, A.; Nand, M.; Sharma, P.; Samant, M.; Pande, V.; Chandra, S., *PLoS One.,* **2021**, *16* (6), e0252759.
25. Din, M. I.; Nabi, A. G.; Rani, A.; Aihetasham, A.; Mukhtar, M., *Environ. Nanotechnology, Monit. Manag.*, **2018**, *9*, 29–36.
26. Sudhasree, S.; Shakila Banu, A.; Brindha, P.; Kurian, G. A., *Toxicol. Environ. Chem.*, **2014**, *96*(5), 743–754.

27. Tanweer, M. S.; Iqbal, Z.; Alam, M., *Langmuir*., **2022**, *38*(29), 8837–8853.
28. Ali, S.; Tanweer, M. S.; Alam, M., *Surfaces and Interfaces*., **2020**, *19*, 100516.
29. Debnath, P.; Mondal, N. K., *Environ. Nanotechnol. Monit. Manag*., **2020**, *14*, 100320.
30. Sachin.; Jaishree.; Singh, N.; Singh, R.; Shah, K.; Shah, B. K., *Chemosphere*., **2023**, *327*, 138497.
31. Fatima, B.; Siddiqui, S.I.; Nirala, R.J.; Vikrant, K.; Kim, K. H.; Ahmad, R.; Chaudhry, S. A., *Environ. Pollut*., **2021**, *271*, 116401.
32. Ghosh, A.; Das, G., *Microporous Mesoporous Mater*., **2020**, *297*, 110039.
33. El-Sharkawy, R. G., *Colloids Surf, A Physicochem Eng Asp*., **2019**, *583*, 123871.
34. Rawat, S.; Singh., *J. Bio Nano Sci*., **2021**, *11*, 1142–1153.
35. Mandal, S.; Alankar, T.; Hughes, R.; Marpu, S.B.; Omary, M.A.; Shi, S.Q., *Surf. Interfaces*., **2022**, *29*, 101797.
36. Gouthaman, A.; Asir, J. A.; Gnanaprakasam, A.; Sivakumar, V. M.; Thirumarimurugan, M.; Ahamed, M. A. R.; Azarudeen, R. S., *J. Hazard. Mater*., **2019**, *373*, 493-503.
37. Joshi, S.; Garg,V.K.; Kataria, N.; Kadirvelu, K., *Chemosphere*., **2019**, *236*, 124280.